

HAT-P-7: A RETROGRADE OR POLAR ORBIT, AND A SECOND PLANET

JOSHUA N. WINN¹, JOHN ASHER JOHNSON^{2,3}, SIMON ALBRECHT¹,
ANDREW W. HOWARD^{4,5}, GEOFFREY W. MARCY⁴, IAN J. CROSSFIELD⁶, MATTHEW J. HOLMAN⁷

Draft version August 12, 2009

ABSTRACT

We show that the exoplanet HAT-P-7b has an extremely tilted orbit, with a true angle of at least 86° with respect to its parent star’s equatorial plane, and a strong possibility of retrograde motion. We also report evidence for a second planet in a more distant orbit. The evidence for the unparallelled orbit and the additional planet is based on precise observations of the star’s apparent radial velocity. The anomalous radial velocity due to rotation (the Rossiter-McLaughlin effect) was found to be a blueshift during the first half of the transit and a redshift during the second half, an inversion of the usual effect, implying that the angle between the sky-projected orbital and stellar angular momentum vectors is 182.5 ± 9.4 . The second planet is implicated by excess radial-velocity variation of the host star over 2 yr. Possibly, the second planet tilted the orbit of the inner planet through a close encounter or the Kozai effect.

Subject headings: planetary systems — planetary systems: formation — stars: individual (HAT-P-7) — stars: rotation

1. INTRODUCTION

In the Solar system, the planetary orbits are well-aligned and prograde, revolving in the same direction as the rotation of the Sun. This fact inspired the “nebular hypothesis” that the Sun and planets formed from a single spinning disk (Laplace 1796). One might also expect exoplanetary orbits to be well-aligned with their parent stars, and indeed this is true of most systems for which it has been possible to compare the directions of orbital motion and stellar rotation (Fabrycky & Winn 2009, Le Bouquin et al. 2009). However, there are at least 3 exoplanets for which the orbit is tilted by a larger angle than any of the planets in the Solar system: XO-3b (Hébrard et al. 2009, Winn et al. 2009a), HD 80606b (Pont et al. 2009, Winn et al. 2009b), and WASP-14b (Johnson et al. 2009).

Still, all of those systems are consistent with prograde orbits, with the largest minimum angle between the stellar-rotational and orbital angular momentum vectors of about 37° , for XO-3b (Winn et al. 2009a). The reason why only the *minimum* angle is known is that the evidence for misalignment is based on the eponymous effect of Rossiter (1924) and McLaughlin (1924), an anomalous Doppler shift observed during planetary transits that is sensitive only to the angle between the *sky projections* of the two vectors. The true spin-orbit angle is undetermined, because of the unknown inclination of the stellar rotation axis with respect to the line of sight.

In this Letter we present evidence for a much larger spin-orbit misalignment, for the exoplanet HAT-P-7b. We find the angle λ between the *sky-projected* angular momentum vectors to be 182.5 ± 9.4 . Furthermore we show that the *true*

angle ψ between those vectors (the stellar obliquity) is likely to be greater than 86° , indicating that the orbit is either retrograde ($\psi > 90^\circ$) or nearly polar ($\psi \approx 90^\circ$). We also present evidence for a second, more distant planet. We present the RV data in § 2, a new transit light curve in § 3, a joint analysis of both types of data in § 4, and a discussion of the results in § 5.

2. RADIAL VELOCITIES

We observed HAT-P-7 with the High Resolution Spectrograph (HIRES) on the Keck I 10m telescope, and the High Dispersion Spectrograph (HDS) on the Subaru 8m telescope. The planet’s discoverers (Pal et al. 2008; hereafter, P08) obtained 8 HIRES spectra in 2007, to which we add 9 spectra from 2009. All but one of the HIRES spectra were acquired outside of transits. Of the 49 HDS spectra, 9 were obtained on 2009 June 17 and 40 were obtained on 2009 July 1. The second of these nights spanned a 4-hour transit.

The instrument settings and observing procedures in both 2007 and 2009 were identical to those used by the California Planet Search (Howard et al. 2009). We placed an iodine gas absorption cell into the optical path, to calibrate the instrumental response and wavelength scale. The radial velocity (RV) of each spectrum was measured with respect to an iodine-free template spectrum, using the algorithm of Butler et al. (2006) with subsequent improvements. Measurement errors were estimated from the scatter in the fits to individual spectral segments spanning a few Angstroms.

2.1. Evidence for a second planet

Fig. 1 shows the RV data outside of transits, fitted with 2 different models. The first model is a single Keplerian orbit, representing the signal of the known planet. The second model has an extra adjustable parameter $\dot{\gamma}$ representing a constant radial acceleration of the star. The second model gives a better fit to the data, with a root-mean-squared (rms) residual of 7 m s^{-1} as compared to 21 m s^{-1} for the first model. The HIRES RVs from 2009 are systematically redshifted by approximately 40 m s^{-1} compared to RVs from 2007 at the same orbital phase. This shift is highly significant, as the CPS has previously demonstrated a long-term stability of 2 m s^{-1}

¹ Department of Physics, and Kavli Institute for Astrophysics and Space Research, Massachusetts Institute of Technology, Cambridge, MA 02139

² Institute for Astronomy, University of Hawaii, Honolulu, HI 96822

³ NSF Astronomy and Astrophysics Postdoctoral Fellow

⁴ Department of Astronomy, University of California, Mail Code 3411, Berkeley, CA 94720

⁵ Townes Postdoctoral Fellow, Space Sciences Laboratory, University of California, Berkeley, CA 94720

⁶ Department of Physics and Astronomy, University of California, Los Angeles, CA 90095

⁷ Harvard-Smithsonian Center for Astrophysics, 60 Garden St., Cambridge, MA 02138

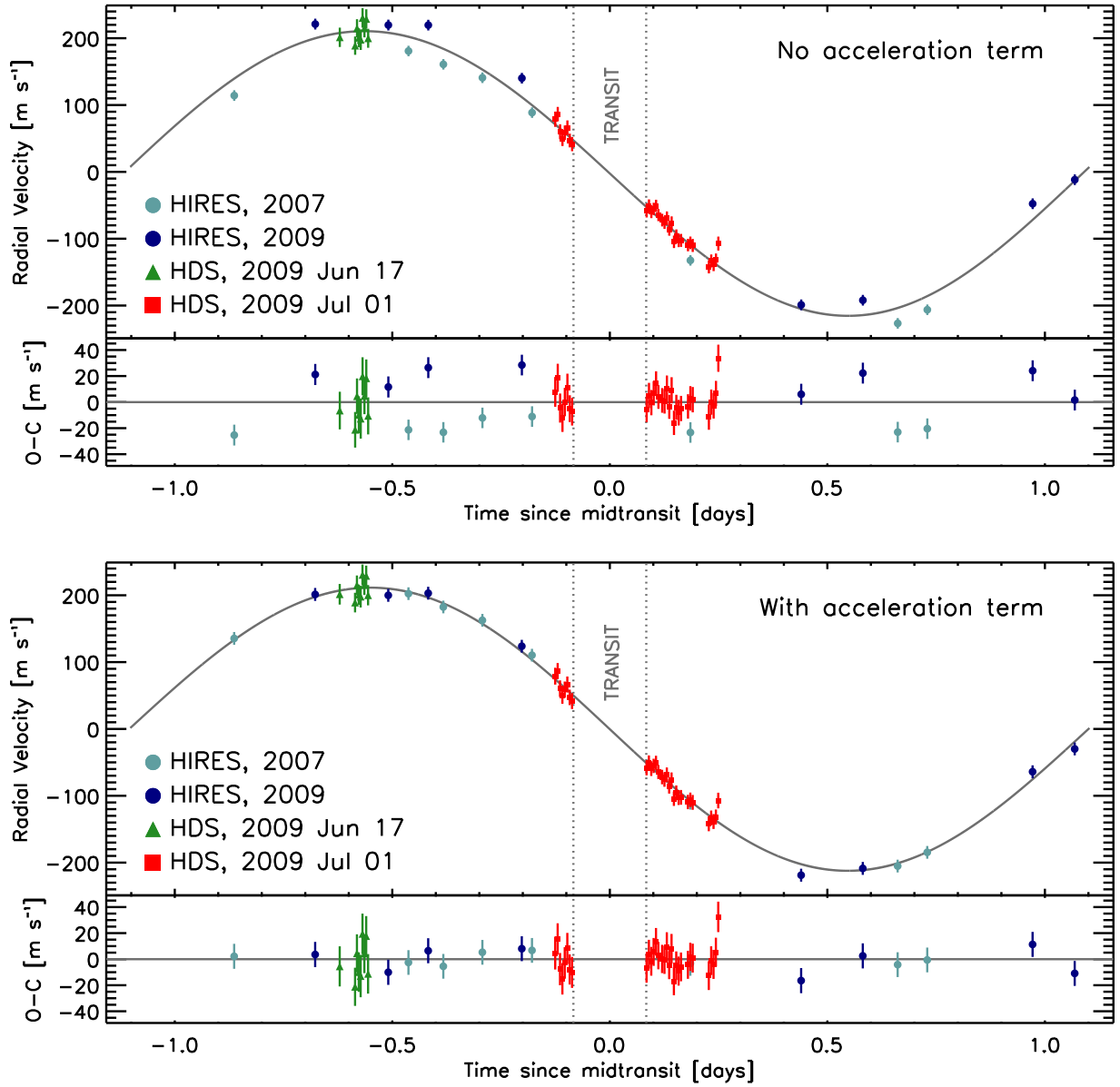


FIG. 1.— **Radial velocity (RV) variation of HAT-P-7 outside of transits.** In the top panel, the RVs are plotted versus orbital phase, assuming a single Keplerian orbit. In the bottom panel, the orbital model has an extra parameter $\dot{\gamma}$ representing a constant radial acceleration, possibly due to a second planet.

or better using HIRES and the same reduction codes used here (Howard et al. 2009).

This RV trend is evidence for an additional orbiting companion. Given the limited time coverage of our observations (two clusters of points separated by 2 yr), the data are compatible with nearly any period longer than a few months. A constant acceleration is the simplest model that fits the excess RV variability, and under that assumption we may give an order-of-magnitude relation relating $\dot{\gamma}$ to some properties of the companion,

$$\frac{M_c \sin i_c}{a_c^2} \sim \frac{\dot{\gamma}}{G} = (0.121 \pm 0.014) M_{\text{Jup}} \text{ AU}^{-2}, \quad (1)$$

where M_c is the companion mass, i_c its orbital inclination relative to the line of sight, a_c its orbital distance, and the numerical value is based on our model-fitting results (see § 4).

2.2. Evidence for a spin-orbit misalignment

Fig. 2 shows the transit data of 2009 July 1, after subtracting the orbital RV as computed from the best-fitting model including $\dot{\gamma}$. We interpret the “anomalous” RV variation during the transit as the Rossiter-McLaughlin (RM) effect, the asymmetry in the spectral lines due to the partial eclipse of the rotating photosphere. In the context of eclipsing binary stars, the RM effect was predicted by Holt (1893) and observed definitively by Rossiter (1924) and McLaughlin (1924). For exoplanets, the RM effect was first observed by Queloz et al. (2000), and its use in assessing spin-orbit alignment was expounded by Ohta et al. (2005) and Gaudi & Winn (2007).

A transiting planet in a well-aligned prograde orbit would first pass in front of the blueshifted (approaching) half of the star, causing the starlight to be anomalously redshifted. Then, the planet would cross to the redshifted (receding) half of the star, causing an anomalous blueshift. In contrast, Fig. 2 shows a blueshift followed by a redshift: an inversion of the effect just described. We may conclude, even without any modeling, that the orbital “north pole” and the stellar “north pole” point in nearly opposite directions on the sky.

3. PHOTOMETRY

For a quantitative analysis of the RM effect we wanted to model both the photometric and spectroscopic transit signals. For this purpose we supplemented the RV data with the most precise transit light curve available to us, shown in Fig. 3. This light curve is based on observations on UT 2008 Sep 22 in the Sloan i bandpass, with the Fred L. Whipple 1.2m telescope and KeplerCam detector, under the auspices of the Transit Light Curve project (Holman et al. 2006, Winn et al. 2007).

Reduction of the CCD images involved standard procedures for bias subtraction and flat-field division. Differential aperture photometry was performed for HAT-P-7 and 7 comparison stars. No evidence was found for time-correlated noise using the “time-averaging” method of Pont et al. (2006), as implemented by Winn et al. (2009c). The data shown in Fig. 3 were corrected for differential extinction as explained in § 4.

4. JOINT ANALYSIS

We fitted a model to the photometric and RV data in order to derive quantitative constraints on the angle λ between the sky projections of the orbital and stellar-rotational angular momentum vectors. This angle is defined such that $\lambda = 0^\circ$ when the sky-projected vectors are parallel and $\lambda = 180^\circ$ when they are antiparallel. Our model for the RM effect, shown in

Fig. 2, was based on the technique of Winn et al. (2005): we simulated spectra exhibiting the RM effect at various transit phases, and then measured the apparent RV of the simulated spectra using the same algorithm used on the actual data. This allowed us to relate the anomalous RV to the parameters and positions of the star and planet.

The RV model was the sum of the line-of-sight component of the Keplerian orbital velocity, plus the anomalous RV due to the RM effect. The photometric model was based on the analytic equation for the intensity of a quadratically limb-darkened disk with a circular obstruction (Mandel & Agol 2002). As a compromise between fixing the limb-darkening coefficients u_1 and u_2 at theoretically calculated values, and giving them complete freedom, we fixed $u_1 - u_2$ at the tabulated value of 0.3846 (Claret 2004) and allowed $u_1 + u_2$ to be a free parameter. We also included a free parameter for the coefficient of differential airmass extinction between HAT-P-7 and the ensemble of comparison stars.

We determined the best values of the model parameters and their 68.3% confidence limits using a Markov Chain Monte Carlo algorithm, as described in our previous works (see, e.g., Winn et al. 2009a). The likelihood function was given by $\exp(-\chi^2/2)$ with

$$\chi^2 = \sum_{i=1}^{N_f} \left[\frac{f_i(\text{obs}) - f_i(\text{calc})}{\sigma_{f,i}} \right]^2 + \sum_{i=1}^{N_v} \left[\frac{v_i(\text{obs}) - v_i(\text{calc})}{\sigma_{v,i}} \right]^2, \quad (2)$$

in a self-explanatory notation, with $\sigma_{f,i}$ chosen to be 0.00136, and $\sigma_{v,i}$ chosen to be the quadrature sum of the RV measurement error and a “stellar jitter” term of 9.3 m s^{-1} . These choices led to $\chi^2 = N_{\text{dof}}$ for the minimum- χ^2 model. A Gaussian prior constraint was imposed upon the orbital period based on the precise measurement of P08.

Table 1 gives the results for the model parameters. In particular, the result for λ is $182.5 \pm 9.4 \text{ deg}$, close to antiparallel, as anticipated from the qualitative discussion of § 2.

5. DISCUSSION

Our finding for λ is strongly suggestive of retrograde motion, in which the orbital motion and stellar rotation are in opposite directions. However, it must be remembered that λ refers to the angle between the *sky-projected* angular momentum vectors. The true angle ψ between the vectors is given by

$$\cos \psi = \cos i_* \cos i + \sin i_* \sin i \cos \lambda, \quad (3)$$

where i and i_* are the line-of-sight inclinations of the orbital and stellar angular momentum vectors, respectively. Although i is known precisely from the transit data, i_* is unknown.

Supposing i_* to be drawn from an “isotropic” distribution (uniform in $\cos i_*$), our data demand that $\psi > 86.3^\circ$ with 99.73% confidence. Thus, under this assumption, a retrograde orbit ($\psi > 90^\circ$) is strongly favored, although a nearly-polar and barely-prograde orbit cannot be ruled out.

In fact there is circumstantial evidence that i_* is small and consequently the orbit of HAT-P-7b is nearly polar ($\psi \approx 90^\circ$). The star’s projected rotation rate is unusually low for such a hot star: $v \sin i_* = 4.9_{-0.9}^{+1.2} \text{ km s}^{-1}$ in our model, or $3.8 \pm 0.5 \text{ km s}^{-1}$ based on the line profile analysis of P08; and $T_{\text{eff}} = 6350 \pm 80 \text{ K}$ according to P08. In the SPOCS catalog of dwarf stars with well-determined spectroscopic properties (Valenti & Fischer 2005), only 2 of 37 stars with $T_{\text{eff}} = 6350 \pm 100 \text{ K}$ have $v \sin i_* < 4.9 \text{ km s}^{-1}$.

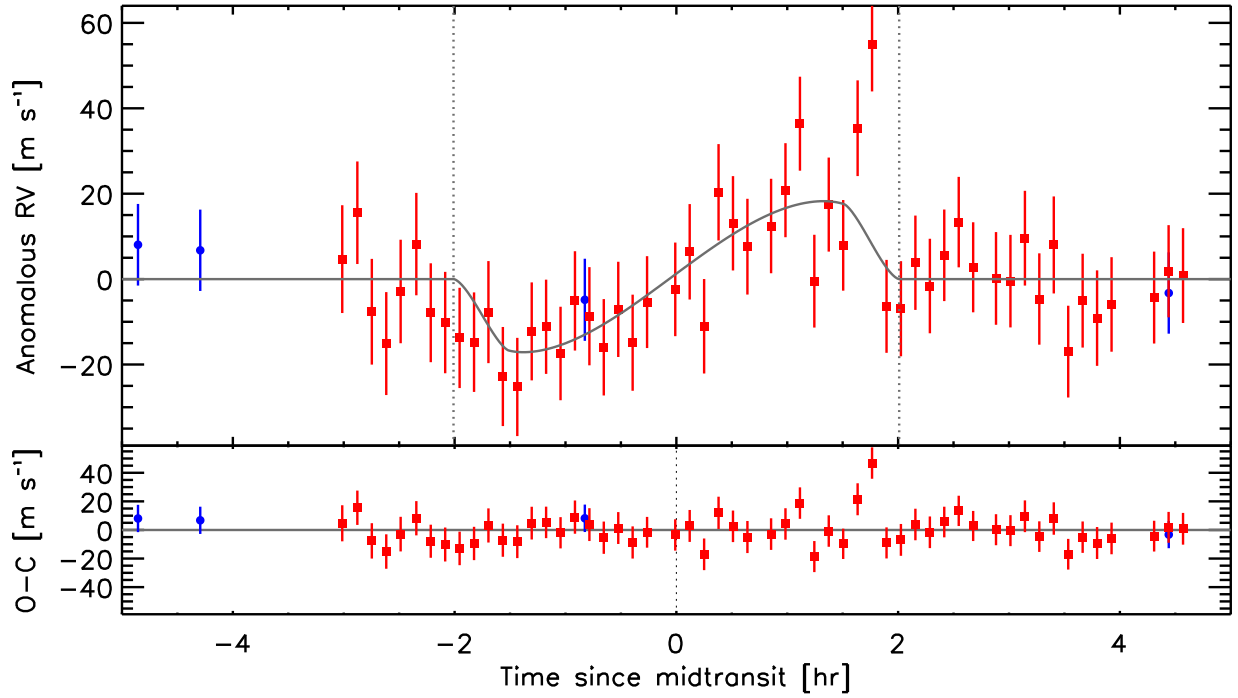


FIG. 2.— **The anomalous RV of HAT-P-7**, defined as the RV determined by our Doppler code minus the orbital RV calculated according to the best-fitting model. The anomalous RV is a blueshift in the first half of the transit, and a redshift in the second half of the transit, demonstrating that the sky projections of the orbital and stellar angular momentum vectors point in opposite directions on the sky plane. The red squares are HDS data from 2009 July 1, and the blue circles are HRES data obtained on various nights in 2007 and 2009. The gray line shows the best-fitting model.

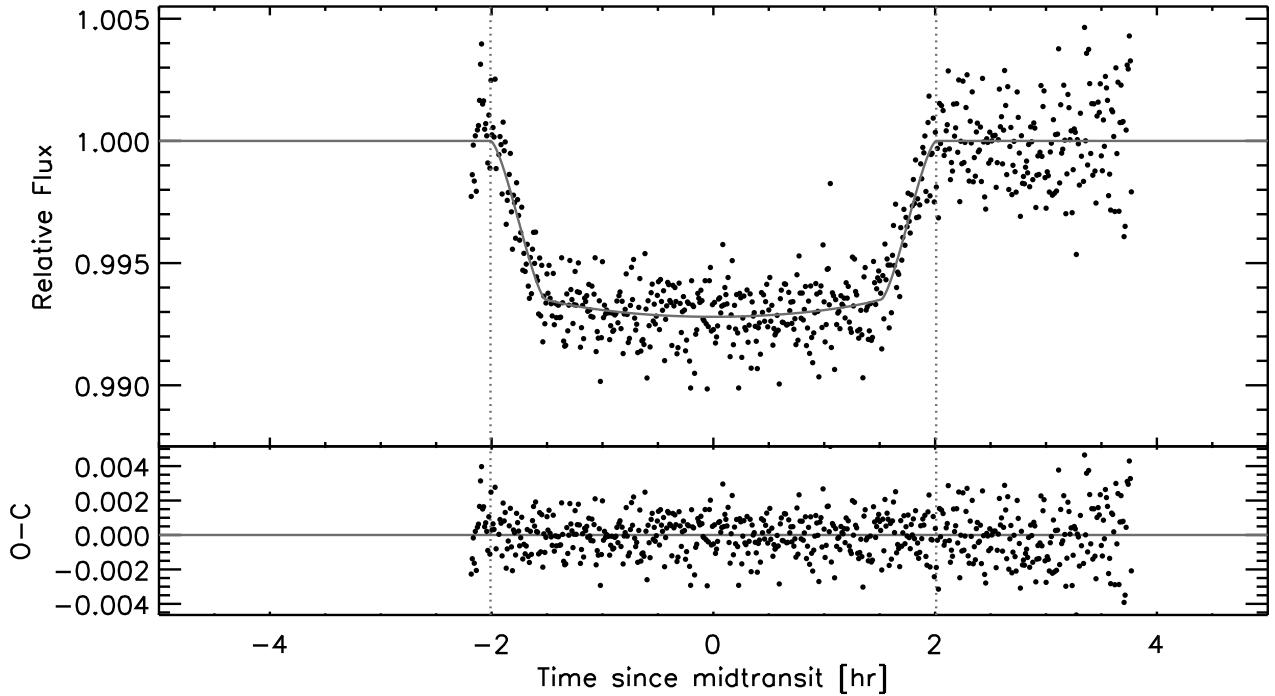


FIG. 3.— **The photometric transit of HAT-P-7**, observed in the Sloan *i* band with the FLWO 1.2m telescope and KeplerCam. The gray line shows the best fitting model.

Based on this catalog, the mean rotation rate ν for such hot stars is about 15 km s^{-1} . As an alternate approach to constraining ψ , we assumed the rotation velocity ν is drawn from a Gaussian distribution with mean 15 km s^{-1} and standard deviation 3 km s^{-1} . The result is $\psi = 94.6^{+5.5}_{-3.0} \text{ deg}$ with 68.3% confidence, and $\psi > 86^\circ$ with 99.73% confidence. This analysis favors nearly-polar and retrograde orbits. However, one wonders whether HAT-P-7 should be expected to have a “typical” rotation rate, given the existence of its short-period planet on a bizarre orbit.

Determining i_* directly may be possible by measuring and interpreting asteroseismological oscillations (Gizon & Solanki 2003), or photometric modulations produced by starspots (see, e.g., Henry & Winn 2008). By good fortune, HAT-P-7 is in the field of view of the *Kepler* satellite, which is capable of extremely precise photometry and may be able to accomplish these tasks (Borucki et al. 2009).

The extraordinary orbit of HAT-P-7b presents an extreme case for theories of planet formation and subsequent orbital evolution. HAT-P-7b is a “hot Jupiter”, and presumably migrated inward toward the star after its formation. A prevailing migration theory involves tidal interactions with the protoplanetary disk, but such interactions would probably not perturb the initial coplanarity of the system, and might even bring the system into closer alignment (Lubow & Ogilvie 2001, Cresswell et al. 2007). More promising to explain HAT-P-7b are scenarios involving few-body dynamics, as those scenarios are expected to produce misalignments. In one scenario, close encounters between planets throw a planet inward, where its orbit is ultimately shrunk and circularized by tidal dissipation (Chatterjee et al. 2008, Jurić & Tremaine 2008). Another idea is based on the Kozai (1962) effect, whereby the gravitational force from a distant body on a highly inclined orbit strongly modulates an inner planet’s orbital eccentricity and inclination (Fabrycky & Tremaine 2007). Recent calculations suggested that a combination of planet-planet scattering and the Kozai effect can lead to retrograde orbits (Nagasawa et al. 2008).

The prospect of explaining HAT-P-7b’s orbit through few-body dynamics lends extra importance to confirming the existence of the second planet and determining its orbital parameters. If it is confirmed, then HAT-P-7b will be only the second known case of a transiting planet accompanied by another planet, the first being HAT-P-13b (Bakos et al. 2009). Such systems are highly desirable because the unusually precise measurements enabled by transit observations can be used to determine whether the orbits are coplanar and give clues about the system’s dynamical history (Fabrycky 2009).

We are grateful to Yasushi Suto and Ed Turner for stimulating our interest in this subject; Mark Everett, Howard Isaacson, and Zach Gazak for observing help; Gáspár Bakos and Joel Hartman for help obtaining telescope time; Eric Gaidos and Debra Fischer for trading telescope time on short notice; and Hector Balbontin for hospitality at Las Campanas Observatory where this manuscript was written. Some of the data presented herein were obtained at the W.M. Keck Observatory, which is operated as a scientific partnership among the California Institute of Technology, the University of California, and the National Aeronautics and Space Administration, and was made possible by the generous financial support of the W.M. Keck Foundation. We extend special thanks to those of Hawaiian ancestry on whose sacred mountain of Mauna Kea we are privileged to be guests. Without their generous hospitality, the Keck observations presented herein would not have been possible. J.A.J. gratefully acknowledges support from the NSF Astronomy and Astrophysics Postdoctoral Fellowship program (grant no. AST-0702821). S.A. acknowledges the support of the Netherlands Organisation for Scientific Research (NWO). J.N.W. gratefully acknowledges support from the NASA Origins program through awards NNX09AD36G and NNX09AB33G, and from a MIT Class of 1942 Career Development Professorship.

Facilities: Subaru (HDS), Keck:I (HIRES), FLWO:1.2m (Keplercam)

REFERENCES

- Bakos, G. A., et al. 2009, arXiv:0907.3525
 Borucki, W. J., et al. 2009, *Science*, 325, 709
 Butler, R. P., et al. 2006, *ApJ*, 646, 505
 Chatterjee, S., Ford, E. B., Matsumura, S., & Rasio, F. A. 2008, *ApJ*, 686, 580
 Claret 2004, *A&A*, 428, 1001
 Cresswell, P., Dirksen, G., Kley, W., & Nelson, R. P. 2007, *A&A*, 473, 329
 Fabrycky, D., & Tremaine, S. 2007, *ApJ*, 669, 1298
 Fabrycky, D. C., & Winn, J. N. 2009, *ApJ*, 696, 1230
 Fabrycky, D. C. 2009, in *Proc. IAU Symposium 253*, eds. F. Pont, D.D. Sasselov, & M.J. Holman (Cambridge: CUP), 173
 Gaudi, B. S. & Winn, J. N. 2007, *ApJ*, 655, 550
 Gizon, L., & Solanki, S. K. 2003, *ApJ*, 589, 1009
 Hébrard, G., et al. 2008, *A&A*, 488, 763
 Henry, G. W., & Winn, J. N. 2008, *AJ*, 135, 68
 Holman, M. J., et al. 2006, *ApJ*, 652, 1715
 Holt, J. R. 1893, *Astronomy and Astro-Physics*, 12, 646
 Howard, A. W., et al. 2009, *ApJ*, 696, 75
 Johnson, J. A., Winn, J. N., Albrecht, S., Howard, A. W., Marcy, G. W., & Gazak, J. Z. 2009, arXiv:0907.5204
 Jurić, M., & Tremaine, S. 2008, *ApJ*, 686, 603
 Kozai, Y. 1962, *AJ*, 67, 591
 Laplace, P. S. 1796, *Exposition du système du monde* (Paris: Cercle-Social)
 Le Bouquin, J.-B., Absil, O., Benisty, M., Massi, F., Mérand, A., & Steff, S. 2009, *A&A*, 498, L41
 Lubow, S. H., & Ogilvie, G. I. 2001, *ApJ*, 560, 997
 Mandel, K., & Agol, E. 2002, *ApJ*, 580, L171
 McLaughlin, D. B. 1924, *ApJ*, 60, 22
 Nagasawa, M., Ida, S., & Bessho, T. 2008, *ApJ*, 678, 498
 Ohta, Y., Taruya, A., & Suto, Y. 2005, *ApJ*, 622, 1118
 Pál, A., et al. 2008, *ApJ*, 680, 1450
 Pont, F., Zucker, S., & Queloz, D. 2006, *MNRAS*, 373, 231
 Pont, F., et al. 2009, *A&A*, 502, 695
 Queloz, D., Eggenberger, A., Mayor, M., Perrier, C., Beuzit, J. L., Naef, D., Sivan, J. P., & Udry, S. 2000, *A&A*, 359, L13
 Rossiter, R. A. 1924, *ApJ*, 60, 15
 Valenti, J. A., & Fischer, D. A. 2005, *ApJS*, 159, 141
 Winn, J. N., et al. 2005, *ApJ*, 631, 1215
 Winn, J. N., Holman, M. J., & Fuentes, C. I. 2007, *AJ*, 133, 11
 Winn, J. N., et al. 2009a, *ApJ*, 700, 302
 Winn, J. N., et al. 2009b, *ApJ*, submitted [arXiv:0907.5205]
 Winn, J. N., et al. 2009c, *ApJ*, 693, 794

TABLE 1
MODEL PARAMETERS FOR HAT-P-7B

Parameter	Value
Orbital period, P [d]	2.2047304 ± 0.0000024
Midtransit time [HJD]	$2,454,731.67929 \pm 0.00043$
Transit duration (first to fourth contact) [hr]	4.006 ± 0.064
Transit ingress or egress duration [hr]	$0.474^{+0.061}_{-0.093}$
Planet-to-star radius ratio, R_p/R_*	$0.0834^{+0.0012}_{-0.0021}$
Orbital inclination, i [deg]	$80.8^{+2.8}_{-1.2}$
Scaled semimajor axis, a/R_*	$3.82^{+0.39}_{-0.16}$
Transit impact parameter	$0.618^{+0.039}_{-0.149}$
Velocity semiamplitude, K [m s ⁻¹]	211.8 ± 2.6
Upper limit on eccentricity (99.73% conf.)	0.039
$e \cos \omega$	-0.0019 ± 0.0077
$e \sin \omega$	0.0037 ± 0.0124
Velocity offset, Keck/HIRES [m s ⁻¹]	-51.2 ± 3.6
Velocity offset, Subaru/HDS [m s ⁻¹]	-4.8 ± 2.5
Constant radial acceleration $\dot{\gamma}$ [m s ⁻¹ yr ⁻¹]	21.5 ± 2.6
Projected stellar rotation rate, $v \sin i_*$ [km s ⁻¹]	$4.9^{+1.2}_{-0.9}$
Projected spin-orbit angle, λ [deg]	182.5 ± 9.4